Int. J. Heat Mass Transfer. Vol. 26, No. 4, pp. 597–605, 1983
Printed in Great Britain

0017-9310/83/040597-09 $03.00/0
Pergamon Press Ltd.

HEAT TRANSFER AND FLOW CHARACTERISTICS OF TWO-PHASE TWO-COMPONENT ANNULAR FLOW

K. SUZUKI, Y. HAGIWARA and T. SATO
Department of Mechanical Engineering, Kyoto University, Kyoto 606, Japan

Abstract—Employing a simple model for the wave effects on momentum, heat and mass transfer, a theory is proposed for the calculation of heat transfer coefficient and flow characteristics of two-phase two-component annular flow. Theoretical results agree reasonably well with the experimental data obtained for a wavy-laminar thin liquid film heated at low heat flux.

(*Received* 12 *May* 1982)

NOMENCLATURE

B, mass transfer number;
B_h, non-dimensional mass transfer contribution to heat transfer;
C_f, skin-friction coefficient;
C_p, specific heat at constant pressure;
F, average number rate of waves;
f, friction factor;
G, mass flow rate per unit area;
g, gravitational acceleration;
H, latent heat of vaporization;
h, bulk mean enthalpy;
J, diffusion mass flux;
L, average wave height;
M, molecular weight;
m_c, local vapour condensation rate;
m_v, evaporation rate per unit surface area;
P, total pressure or partial pressure when suffixed;
Pr, Prandtl number;
q, heat flux;
R, tube radius;
r, radial coordinate;
Sc, Schmidt number;
St, Stanton number;
T, temperature;
u, axial velocity;
u', velocity scale of wave-induced motion;
V, specific volume;
x, axial coordinate;
y^+, universal radial distance.

Greek symbols

α, heat transfer coefficient;
β, non-dimensional parameter defined by equation (20);
κ, von Kármán constant;
μ, viscosity;
ρ, density;
τ, shear stress;
ω_v, mass fraction of vapour.

Subscripts and superscripts

a, air or non-condensable gas;
g, gas phase;
i, interface;
l, liquid phase;
m, reference condition;
t, turbulent;
v, vapour phase;
w, wall;
x, at location x;
0, at location $x = 0$;
~, wave.

1. INTRODUCTION

THE PRESENT study is concerned with heat transfer in a two-phase two-component annular flow in a vertical circular tube. In his recent review on the two-phase two-component heat transfer [1], Michiyoshi pointed out that the effects of a wavy interface structure on heat transfer have not been clarified sufficiently. This article proposes a theory for the calculation of heat transfer and flow characteristics based on a simple model for the wave effects. The numerical results obtained will be compared with the experimental data obtained previously [2]. The comparison covers the heat transfer coefficient, the axial pressure gradient and the average liquid film thickness.

Two-phase annular flow is characterized by a phase interface separating the thin liquid film from the gas flow in the core region. This phase sometimes carries dispersed liquid droplets. The interface is often wavy in nature. The waves appearing on the liquid surface exert influence on the momentum, heat and mass transfer. These wave effects are important in two-component annular flow and in other types of two-phase flow separated by a continuous interface. For this reason the following discussion of previous works on this subject will sometimes go beyond the specific problem concerned in this paper.

For heat transfer in a two-phase two-component annular flow, several experiments have been conducted [3–7]. Apart from differences in tube position (horizontal or vertical), a common feature of these studies is that attention was paid to the case of thick liquid film or the case when the liquid film Reynolds number is higher than its critical value. Information about the heat transfer for thin liquid films is scarce.

Additionally, a study of a thin liquid film offers a better chance to obtain basic knowledge of wave effects: because turbulence is not expected to exist in the liquid film, wave effects are not blurred by the effect of intrinsic liquid-phase turbulence. For example in ref. [2], conspicuous heat transfer augmentation has been found to be caused by the onset of disturbance waves at low liquid film Reynolds numbers. One of the purposes of this paper is to explain this augmentation theoretically.

Among previous theoretical approaches, Pletcher and McManus [8] have presented a means for the prediction of two-phase two-component annular flow heat transfer. Their work is similar in some sense to studies [9-12] for other types of two-phase heat transfer. These works are again concerned with turbulent liquid films. The wave effect has been taken into account in these works only *indirectly*. Interface shear stress or pressure drop under the wave effect has been deduced separately, for example with an empirical formula expressed in terms of the Lockhart–Martinelli parameter. The present study presents a theory for the prediction both of heat transfer coefficient and flow characteristics. For this purpose a model must be introduced to express the wave effect *directly*.

In theoretical approaches to the liquid film flow and related heat transfer, the wave effect is usually not distinguished from the intrinsic turbulence. However, in their paper on the film-wise condensation in a vertical tube, Blangetti and Schlünder [12] tried to separate the wave effect from the turbulence effect. A similar attempt is made in the present study. The thin liquid film discussed in this paper may correspond to the wavy-laminar liquid film in their terminology. To the present authors' knowledge, the modelling of wave effects in this sense has not been discussed thoroughly. Brumfield *et al.* [13] introduced a model for wave effects and had fair success in correlating gas absorption data in falling liquid films. Since the gas phase resistance is not important in this particular problem their model does not provide any information about the wave effect on gas phase transport phenomena. Gas phase resistance is crucial in the present problem. Levy and Healzer [14] reported recently a theory for annular flow assuming a transition layer between the base and the top of waves but the wave effect was not treated directly. In the present study, a simple model, similar in form to a turbulence model called the Prandtl–Kolmogoroff hypothesis, is tested. This does not require the liquid film flow to be turbulent. The length and velocity scales of turbulence in the original model are replaced by their wave counterparts in the present study. Since the liquid film is essentially in a laminar state no attention is paid to the suppression of turbulence owing to interfacial waves or surface tension mentioned in the ref. [12, 15]. Needless to say, the gas phase flow is of higher velocity, so that it is turbulent. This higher velocity is required to generate the disturbance waves on the interface at quite a low liquid film Reynolds number.

2. ASSUMPTIONS, FORMULATION AND CALCULATION PROCEDURE

2.1. *Main assumptions*

Two phase flow heat transfer is complicated by the effects of many factors. In attempting to speculate under which particular conditions a theory being developed might be valid, it may be worthwhile to first mention the main assumptions to be used.

First of all, the wall heat flux is assumed to be low enough so that evaporation does not significantly affect the gas phase flow pattern. Otherwise, the gas phase turbulence would be affected by the transpiration effect [16, 17] and by the flow acceleration due to the rapid increase of gas phase velocity [18]. This assumption, however, does not contradict the importance of the mass transfer effect on heat transfer [8, 19]. This will be easily understood if two parameters B and B_h, defined below, are compared with each other.

$$B = \frac{m_v u_{gm}}{\tau_w} \cong \frac{m_v}{\rho_{gm} u_{gm}} \frac{8}{f} \ll 1 \tag{1}$$

$$B_h = \frac{H m_v}{g_w} = \frac{\rho_{gm} u_{gm}}{\rho_m u_m} \frac{C_f}{2St} B \frac{H}{C_{pm}(T_w - T_m)}. \tag{2}$$

Since the Kutatelatze number $C_{pm}(T_w - T_m)/H$ can be small, B_h is likely to be much larger than B. Thus, mass transfer can play an important role in the overall heat transfer even if it does not affect the flow pattern significantly. The mass transfer problem of liquid vapour is complicated by the occurrence of vapour condensation in the core region. Here it is assumed that the liquid vapour is in saturated condition everywhere at the local gas phase temperature. This assumption will later be found to be effective in removing the difficulty associated with vapour condensation.

As mentioned before, the gas phase velocity is required to be high but the disturbance waves are presumed not to produce a significant amount of droplet entrainment. Therefore, the effect of droplets on overall momentum, heat and mass transfer are ignored. Any droplets suspended in the gas phase flow are only assumed to be effective in preventing the occurrence of liquid vapour supersaturation.

In the following sections, a theory suitable for fully developed flow conditions is described that can be extended to a form useful for either thermally or hydrodynamically developing flow conditions. In the experiments presented in ref. [2], the heat transfer coefficient defined below was found to distribute almost uniformly along the tube axis except in the inlet region, i.e.

$$\alpha = \frac{q_w}{T_w - T_c} \tag{3}$$

where T_c is the fluid temperature at the tube axis. This implies the attainment of a state close to the fully developed condition. The prediction of such a state accords with the low wall heat flux assumed earlier, as will be found later.

2.2. *Basic equations*

The governing equations of the present problem may be written as follows:

in the liquid film ($r_i \leqslant r \leqslant R$)

$$0 = -\frac{dP}{dx} + \frac{1}{r}\frac{d}{dr}(r\tau_l) + \rho_l g \tag{4}$$

$$\rho_l C_{pl} u_l \frac{\partial T_l}{\partial x} = -\frac{1}{r}\frac{d}{dr}(rq_l) \tag{5}$$

in the gas phase core region ($0 \leqslant r \leqslant r_i$)

$$0 = -\frac{dP}{dx} + \frac{1}{r}\frac{d}{dr}(r\tau_g), \tag{6}$$

$$\rho_g C_{pg} u_g \frac{\partial T_g}{\partial x} = -\frac{1}{r}\frac{d}{dr}(rq_g) + Hm_c \tag{7}$$

$$\rho_g u_g \frac{\partial \omega_v}{\partial x} = -\frac{1}{r}\frac{d}{dr}(rJ_v) - m_c \tag{8}$$

where the enthalpy change due to pressure variation and the diffusion-thermo effect have been neglected. The latter may be consistent with another assumption about the Prandtl and the Schmidt numbers to be introduced later. The momentum, heat and mass fluxes appearing in the above equations are expressed in the following forms:

$$\tau_l = (\mu_l + \tilde{\mu}_l)\frac{du_l}{dr},$$

$$q_l = -\left(\frac{\mu_l C_{pl}}{Pr_l} + \frac{\tilde{\mu}_l C_{pl}}{\tilde{P}r_l}\right)\frac{\partial T_l}{\partial r}, \tag{9}$$

$$\tau_g = (\mu_g + \tilde{\mu}_g + \mu_t)\frac{du_g}{dr},$$

$$q_g = -\left(\frac{\mu_g C_{pg}}{Pr_g} + \frac{\tilde{\mu}_g C_{pg}}{\tilde{P}r_g} + \frac{\mu_t C_{pg}}{Pr_t}\right)\frac{\partial T_g}{\partial r}, \tag{10}$$

$$J_v = -\left(\frac{\mu_g}{Sc_g} + \frac{\tilde{\mu}_g}{\tilde{S}c_g} + \frac{\mu_t}{Sc_t}\right)\frac{\partial \omega_v}{\partial r}$$

$$= -\left(\frac{\mu_g}{Pr_g} + \frac{\tilde{\mu}_g}{\tilde{P}r_g} + \frac{\mu_t}{Pr_t}\right)\frac{\partial \omega_v}{\partial r} \tag{11}$$

where $\tilde{\mu}_l$ and $\tilde{\mu}_g$ account for the wave effects in the liquid film and in the gas flow, respectively. The expressions for them will be described in the next section. The second expression of equation (11) has been obtained by assuming equality between the Schmidt number and its corresponding Prandtl number. This assumption is approximately valid in the gaseous flow.

2.3. *A model for the wave effects*

As a wave proceeds on the interface, a fluid particle in the liquid film experiences inward and outward radial motion alternately. This means that a portion of liquid relatively hotter and of lower momentum may move inward and be cooled and accelerated. The portion of liquid thus cooled and accelerated is then fed back toward the tube wall. This radial motion is expected to enhance the heat and momentum transfer in the liquid film. Although this wave-induced motion is not actually turbulent the mechanism of heat and momentum transfer enhancement mentioned above is analogous to that caused by turbulent eddy motion. Thus, a model for the wave viscosity $\tilde{\mu}_l$ in parallel with the Prandtl–Kolmogoroff hypothesis [20] is proposed here. That is,

$$\tilde{\mu}_l^* = C\rho_l u' \Lambda \tag{12}$$

where u' and Λ are the velocity and length scales of the wave-induced motion, respectively, and C is an adjustable constant. In the present study, Λ is replaced by the stroke of the wave-induced motion, i.e. the average wave height L. The velocity scale is given by the ratio $(L\tilde{u}/b)$, where $\tilde{u}$ is the wave speed and b the mean base breadth of waves. This is the velocity necessary for a fluid particle to complete half of the average radial motion during the period between the arrival of a wave front and the departure of the wave. The liquid film experiences the above wave effect only in a fraction of time expressed by the ratio (b/p), where p is the averaged pitch of waves. In the remaining time fraction $(1-b/p)$, the effective viscosity is just equal to μ_l, the liquid viscosity. Then the average effective viscosity is given as follows:

$$\mu_l + \tilde{\mu}_l = \frac{b}{p}\left(\mu_l + C\rho_l \frac{L^2\tilde{u}}{b}\right) + \left(1 - \frac{b}{p}\right)\mu_l$$

$$= \mu_l + C\rho_l L^2 F \tag{13}$$

where F is the average number rate of waves passing a cross sectional plane. A schematic illustration of the present model is shown in Fig. 1. The radial wave-induced motion must vanish at the wall and should be suppressed close to the wall. Therefore, $\tilde{\mu}_l$ is put equal to zero in the wall region corresponding to the viscous sublayer in a single phase turbulent flow,

$$0 \leqslant y_l^+ = \frac{(\rho_l \tau_w)^{1/2}(R-r)}{\mu_l} \leqslant 5. \tag{14}$$

The radial wave-induced motion also occurs in the gas phase flow. It is assumed to be effective only in that it intermittently breaks up the viscous sublayer in the gas phase flow which should exist near the interface unless waves appear. This idea corresponds to an assumption that the viscous sublayer is replaced by a thin layer where the following virtual viscosity, similar to equation (13), is effective:

$$\mu_g + \tilde{\mu}_g = \frac{b}{p}\left(\mu_g + C\rho_g \frac{L^2\tilde{u}}{b}\right) + \left(1 - \frac{b}{p}\right)\mu_g$$

$$= \mu_g + C\rho_g L^2 F. \tag{15}$$

In this layer, the turbulent viscosity has been put equal to zero and the wave viscosity, $\tilde{\mu}_g$, is assumed to be ineffective outside this layer. Thus, the layer is assumed to extend to a position where the wave effective viscosity, equation (15), and the turbulent effective

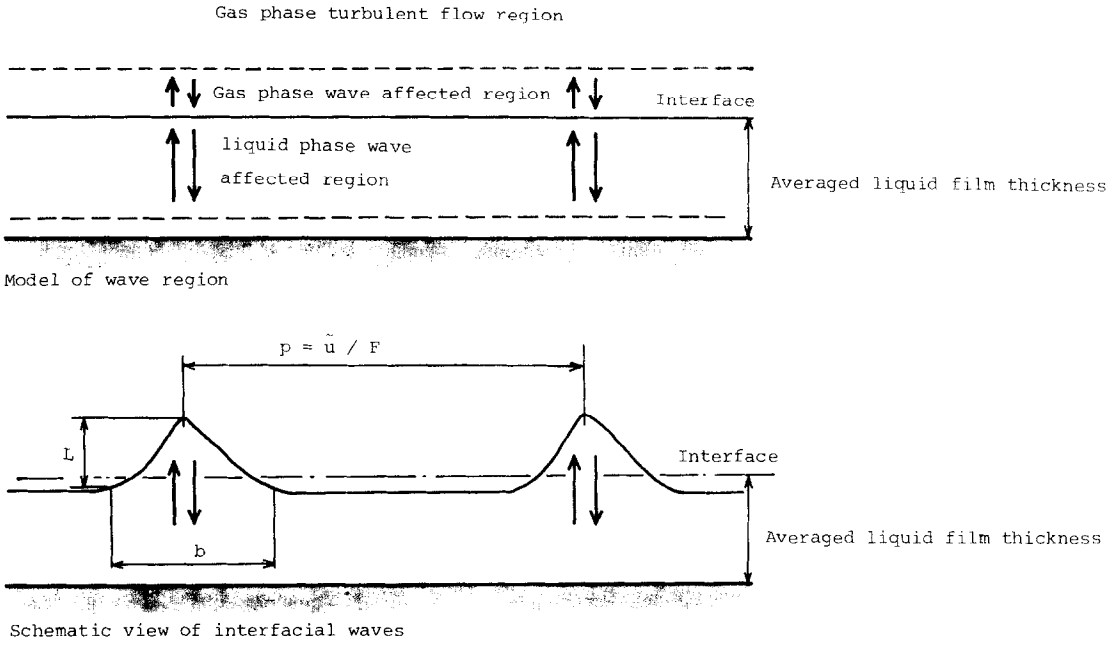

FIG. 1. Schematic illustration of the present wave effect model (lengths not to scale).

viscosity, $(\mu_g+\mu_t)$, coincide with each other. For the evaluation of $(\mu_g+\mu_t)$, the distribution of μ_t is given in the usual way for single phase turbulent flow as follows:

$$0 \leqslant y_g^+ = \frac{(\rho_g \tau_{gi})^{1/2}(r_i - r)}{\mu_g} \leqslant 5, \quad \mu_t = 0,$$

$$5 \leqslant y_g^+ \leqslant 30, \quad \mu_t = \mu_g\left(\frac{y_g^+}{5} - 1\right),$$

$$y_g^+ \geqslant 30, \quad \mu_t = \rho\kappa^2(r_i - r)^2\left|\frac{du_g}{dr}\right|.$$

2.4. *Treatment of mass transfer effect*

Instead of introducing a model for the direct evaluation of m_c appearing in equations (7) and (8), another method will be used in this study. This is a method for the elimination of terms including m_c, and it simplifies the matching condition for the energy equation at the interface. To start with, the Clapeyron–Clausius equation is introduced for saturated liquid vapour,

$$\frac{dP_v}{dT_g} = \frac{H}{T_g V_v} \tag{16}$$

where the specific volume of liquid has been neglected in comparison with the much larger value of V_v. When the partial pressure of liquid vapour P_v is much less than total pressure P, it may be related approximately linearly to the mass fraction of liquid vapour ω_v.

$$\omega_v = \frac{M_v P_v}{M_a(P - P_v) + M_v P_v} \cong \frac{M_v P_v}{M_a P} \tag{17}$$

where the thermally ideal gas law has been assumed. Under the low heat flux assumption, T_g is not expected to vary greatly in either the r direction or along the x axis. The following approximation may then be used for ω_v:

$$\omega_v = \omega_{vm} + \left(\frac{d\omega_v}{dT_g}\right)_m (T_g - T_m) \tag{18}$$

where ω_{vm} and $(d\omega_v/dT_g)_m$ are evaluated at a local reference temperature T_m, to be defined later. Substituting of equations (16)–(18) into equation (8) and using the second expression of equation (11) gives

$$\beta\rho_g C_{pg} u_g \frac{\partial T_g}{\partial x} = \frac{1}{r}\frac{\partial}{\partial r}\left[\beta r\left(\frac{\mu_g C_{pg}}{Pr_g} + \frac{\tilde{\mu}_g C_{pg}}{\tilde{P}r_g} + \frac{\mu_t C_{pg}}{Pr_t}\right)\frac{\partial T_g}{\partial r}\right] - Hm_c \tag{19}$$

where β is a non-dimensional parameter expressing the degree of the mass transfer contribution to heat transfer,

$$\beta = \frac{H^2 M_v}{M_a C_{pg} P T_m V_{vm}} \tag{20}$$

Now the conservation equation for ω_v has been transformed into the differential equation of T_g. From equations (7), (10) and (19), the following simple equation can be derived:

$$\rho_g C_{pg} u_g (1+\beta)\frac{\partial T_g}{\partial x} = \frac{1}{r}\frac{\partial}{\partial r}\left[r(1+\beta) \times \left(\frac{\mu_g C_{pg}}{Pr_g} + \frac{\tilde{\mu}_g C_{pg}}{\tilde{P}r_g} + \frac{\mu_t C_{pg}}{Pr_t}\right)\frac{\partial T_g}{\partial r}\right]. \tag{21}$$

This equation no longer has any terms including m_c and is much easier to solve. The governing equations for combined heat and mass transfer have now been

reduced to a single equation (21) which is in the same form as the energy equation for single-phase flow. This implies that the thermally fully developed state, if actually possible, can be expected to be attained at the low heat flux which has been assumed in the above derivation.

2.5. *Boundary and matching conditions, and calculation procedure*

The boundary conditions adopted at the wall are

$$u_l = 0 \quad \text{and} \quad q_l = q_w \tag{22}$$

and the matching conditions at the interface are,

$$u_{li} = u_{gi},\ T_{li} = T_{gi}$$

and

$$\tau_{li} = \tau_{gi},$$

$$-\left(\frac{\mu_l C_{pl}}{Pr_l} + \frac{\tilde{\mu}_l C_{pl}}{\tilde{P}r_l}\right)\left(\frac{\partial T_l}{\partial r}\right)\Bigg|_i = -(1+\beta)\left(\frac{\mu_g C_{pg}}{Pr_g} + \frac{\tilde{\mu}_g C_{pg}}{\tilde{P}r_g}\right)\left(\frac{\partial T_g}{\partial r}\right)\Bigg|_i. \tag{23}$$

The gas phase temperature gradient at the interface is now clearly seen to be reduced in magnitude by the effect of mass transfer by a factor $1/(1+\beta)$. The remaining boundary conditions on the tube axis are replaced by the overall pressure–force balance and the energy balance expressed by the following equations:

$$\frac{dP}{dx} = \frac{2\tau_w}{R} + \rho_l g\left[1 - \left(\frac{r_i}{R}\right)^2\right], \tag{24}$$

$$q_w = \frac{dT_m}{dx}\left[\int_{r_i}^{R} 2\pi\rho_l C_{pl} u_l r\, dr + (1+\beta)\int_0^{r_i} 2\pi\rho_g C_{pg} u_g r\, dr\right] \tag{25}$$

where the axial gradient of a reference temperature T_m has been equated with $\partial T_g/\partial x$ and $\partial T_l/\partial x$, in accordance with the fully developed state assumption, as follows:

$$\frac{dT_m}{dx} = \frac{\partial T_g}{\partial x} = \frac{\partial T_l}{\partial x}. \tag{26}$$

The reference temperature, T_m, is equated with the equilibrium temperature, introduced by Pletcher and McManus, and defined as

$$2\pi R x q_w = G_{lx}(h_{lx} - h_{l0}) + G_a(h_{ax} - h_{a0}) + \Delta G_v(h_{vx} - h_{l0}) + G_{v0}(h_{vx} - h_{v0}) \tag{27}$$

where h_{lx}, h_{ax} and h_{ax} are the enthalpy at the temperature T_m to be defined at a position x for liquid, air or non-condensable gas and liquid vapour, respectively, and

$$\Delta G_v = \frac{G_a M_v}{M_a P}(P_{vx} - P_{v0}). \tag{28}$$

The above equations are coupled with an overall mass continuity equation for each phase,

$$G_l = \int_{r_i}^{R} 2\pi\rho_l u_l r\, dr, \tag{29}$$

$$G_g = \int_0^{r_i} 2\pi\rho_g u_g r\, dr. \tag{30}$$

These are used in iterative processes to check the validity of assumed values of r_i and τ_w, as described below.

The practical computation starts with the calculation of the liquid phase velocity profile by integrating equation (4) with initially guessed values of r_i and τ_w, and the pressure gradient dP/dx evaluated from equation (24). If the velocity profile obtained satisfies the mass balance equation (29), the calculation proceeds with the integration of equation (6) with τ_{gi} obtained from equation (23). If not, the value of r_i is renewed and the above process is repeated. Equation (30) is used to check the validity of the gas phase velocity profile obtained by the integration of equation (6). If the gas phase velocity profile is not satisfactory, the value of τ_w is changed and the above whole process is repeated. The iterative process is stopped when the two equations (29) and (30) are satisfied within an accuracy of 0.1%. At this stage of the calculation, the integration of equation (21) is started to compute the temperature profile. For heat and mass transfer, $\tilde{P}r$ and Pr_t are all equated with unity in the present calculation. At the end, the heat transfer coefficient, the pressure gradient and the mean liquid film thickness are determined. The numerical computation was made with a FACOM M-200 computer at the Data Processing Centre of Kyoto University.

3. RESULTS AND DISCUSSION

3.1. *Outline of the experiments*

All the experimental data to be compared with the present theory are taken from the ref. [2] except for the pressure gradient, which was obtained in the same experiments but was not included in that report. To show the compatibility between the present theory and the experiments, a brief description of the experimental apparatus used in the study is given here. The test tube is a vertically mounted circular tube of 1850 mm length and 26.3 mm I.D. The air flow coming into the test tube through a contraction nozzle suspends water droplets sprayed with air atomizers located in the contraction nozzle. The main portion of the sprayed water diffuses outward and is deposited on the wall of the contraction nozzle. Thus, an annular liquid film is already formed at the entrance of the test tube, but continuing deposition of the remaining droplets gradually makes the liquid film thicker. However, the thickening rate is low enough in the downstream half of the tube because the portion of liquid flowing in the form of droplets is much smaller than the liquid flow rate in the film. The liquid film is thin enough to remain laminar but disturbance waves can appear on its surface depending on the air flow rate. Droplet entrainment from the crests of

disturbance waves has been checked to be low enough. The air flow has been confirmed to attain a hydrodynamically fully developed state after the point 1200 mm downstream from the tube inlet [21]. In this region, the heat transfer coefficient has been found to distribute almost uniformly. The pressure drop has also been measured in this region. Heat transfer experiments were conducted at two different levels of wall heat flux. The wall heat flux at higher level is almost twice the lower wall heat flux. The difference in wall heat flux means the difference in the mass transfer effect on heat transfer and these data serve as a means of checking the validity of the present method using equation (21).

3.2. *Wave parameters*

In the present calculation, the measured values are used temporarily for the two wave parameters L and F appearing in equations (13) and (15). It is desirable in future to devise general empirical formulae or a theoretical means available for their evaluation. The values used for L and F are listed in Table 1 together with other information, for all the flow rate conditions at which the following comparisons were made. These values were obtained by processing the replayed trace of liquid film thickness δ, measured with a conductance probe and discussed in ref. [2]. The value of F is the average of the time interval between two successive disturbance waves. The disturbance wave was detected with a threshold for the time derivative of the trace of δ, such that $(1/\bar{u})(\mathrm{d}\delta/\mathrm{d}t) > 0.15$. This detection method is based upon a finding that the waves with large amplitude found in the trace seems to be characterized by a rapid increase in height. It is similar to the method used by Sekoguchi *et al.* [22]. L is the averaged value of the amplitude of the detected waves. The amplitude of each wave is defined as the difference between the first maximum height of the wave after its detection and the value of δ at the instant of detection.

Apart from the main aim of the present calculation to evaluate the effect of disturbance waves, the effect of ripple waves was also examined in a preliminary study. For that purpose, two wave parameters L_r and F_r were measured for ripple waves. The values of L_r and F_r were obtained by conditional processing for the non-disturbance-wave portion to the original trace of δ. In contrast to disturbance waves, which appear intermittently, ripple waves appear continuously at the interface, so that $h = p$. Therefore, it may be pertinent to adapt equations (13) and (15) for this particular purpose as follows:

$$\mu_l + \tilde{\mu}_l = \mu_l + C\rho_l L^2 F + C\rho_l L_r^2 F_r,$$

$$\mu_g + \tilde{\mu}_g = \mu_g + C\rho_g L^2 F + C\rho_g L_r^2 F_r.$$

The effect of the last terms of these equations was found to be negligible even compared with the fluid viscosities μ_l and μ_g. This is based on that fact that $L_r \ll L$. Therefore the discussion below is concentrated on the effect of disturbance waves. Different values have been tested for C. The value finally adopted is 1.34 for the values of L and F listed in Table 1.

3.3. *Discussion of results*

Figure 2 shows a comparison of the heat transfer coefficient. The symbols with flag specify data obtained at higher wall heat flux. Some of the plotted points are for the condition when disturbance waves appear on the interface, others are for the condition with ripple waves only. The former corresponds to the group specified as D.W. and the latter group specified as Ripple. The present theory is found to agree very well with the experimental results for all flow rate conditions and at different levels of wall heat flux. While the calculated value of B is around 10^{-2} for all the data plotted, the value of B_h is larger than 0.50 so that the mass transfer effect is crucial in all conditions compared. In the ripple wave condition, the effective viscosity, equation (13), and the virtual viscosity, equation (15), become equal to μ_l and μ_g, respectively. Thus, the good agreement obtained in that condition proves the validity of the present method using equation (21) for mass transfer effect. In the disturbance wave condition, the wave viscosity plays an important role so that the agreement obtained in this condition

Table 1. Wave parameters

G_g (g s^{-1})	Gas phase Reynolds number	G_l (g s^{-1})	Liquid film Reynolds number	L (mm)	F (Hz)	Observed waves
11.5	3.0×10^4	3.33	1.4×10^2	0.075	7.5×10	Ripple
		6.67	2.8×10^2	0.082	6.7×10	Ripple
		10.0	4.2×10^2	0.60	4.4	D.W.
		11.7	5.0×10^2	0.89	4.3	D.W.
15.5	4.0×10^4	3.33	1.4×10^2	0.073	7.9×10	Ripple
		6.67	2.8×10^2	0.080	6.9×10	Ripple
		10.0	4.2×10^2	0.55	5.6	D.W.
		11.7	5.0×10^2	0.81	5.4	D.W.
21.1	5.5×10^4	3.33	1.4×10^2	0.070	8.2×10	Ripple
		6.67	2.8×10^2	0.078	6.9×10	Ripple
		10.0	4.2×10^2	0.43	7.0	D.W.
		11.7	5.0×10^2	0.68	7.1	D.W.

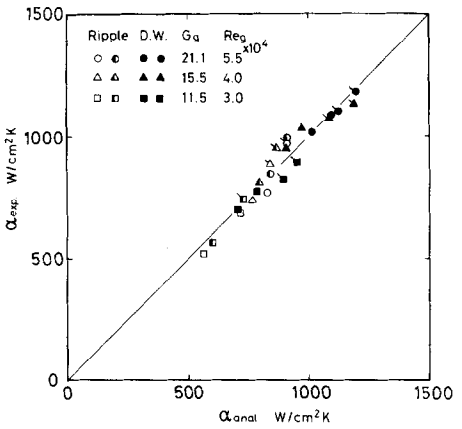

FIG. 2. Comparison of heat transfer coefficient.

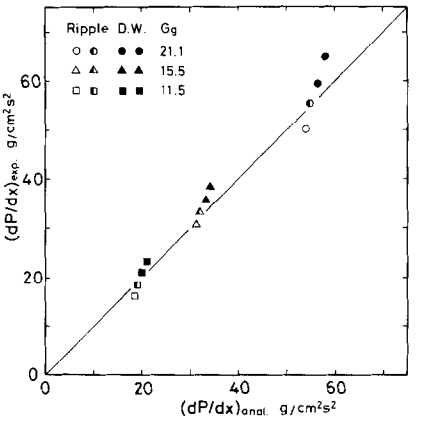

FIG. 4. Comparison of axial pressure gradient.

gives support to the wave effect model adopted in this study, at least for the evaluation of the heat transfer coefficient. This is more clearly demonstrated if Fig. 2 is compared with Fig. 6 (see Appendix).

An example of the calculated radial temperature profile is shown in Fig. 3. The figure shows that the largest heat transfer resistance lies in the gas phase region close to the interface. However, it should be noted that the temperature drop in this region is reduced in magnitude because of the mass transfer effect. If there is no mass transfer, the temperature drop in this region must be much larger. The significance of the mass transfer effect can be guessed from the value of β defined by equation (20). V_{vm} in equation (20) is a sensitive function of the temperature T_m. The reference temperature is affected by the level of the wall heat flux and the inlet condition. The existing empirical formulae for the two-phase two-component heat transfer do not include terms accounting for the inlet temperature. Thus, we should be cautious about the usage of such formulae.

Figure 4 compares the calculated axial pressure gradient with the experimental counterparts. Fairly good agreement is again found between the present theory and the experimental data. But it may be worth noting for future works an incomplete feature of the present results. In the figure, comparisons are made for four different liquid flow rates at each air flow rate G_g. The variation of dP/dx accompanying the change in liquid flow rate is predicted to be smaller than the experimental result. This may be related to the thicker liquid film predicted at large liquid flow rates.

Figure 5 shows a comparison for the mean liquid film thickness. The agreement of this comparison is not bad on the whole, but a discrepancy is found between the present theory and the experiment at larger liquid flow rates or in the condition when disturbance waves appear. The liquid film is then predicted to be thicker than is actually found in the experiments. A thicker liquid film corresponds to a lower liquid velocity, as is easily estimated from the overall mass flow rate restriction. This means a lower wall shear stress and, therefore, a smaller variation of dP/dx with the change in the liquid flow rate. This is the cause of the discrepancy found in Fig. 4. As already found in Fig. 3, the liquid film causes minor heat transfer resistance. Thus, much better agreement has been obtained in the heat transfer coefficient.

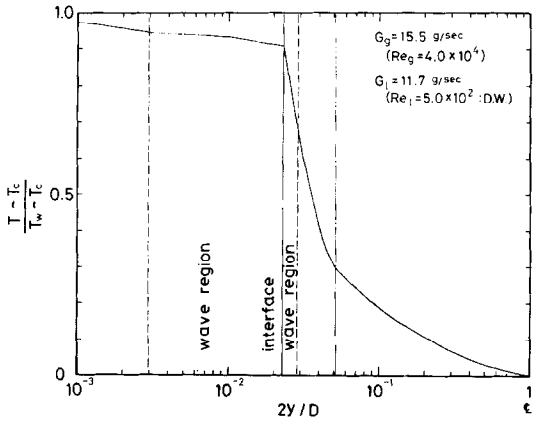

FIG. 3. Calculation profile of temperature.

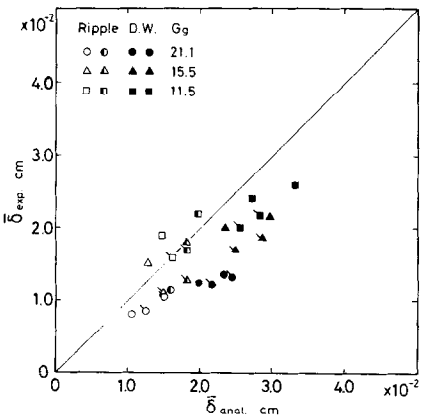

FIG. 5. Comparison of mean film thickness.

4. CONCLUSIONS

A theoretical method has been proposed for the evaluation of heat transfer and flow characteristics of two-phase two-component annular flow with a thin liquid film heated at low heat flux. The present method, introduced to account for the mass transfer effect, has been proved to be valid. Based on this method, a warning has been given on the usage of the existing heat transfer empirical formulae. A simple model for the wave effect employed in this study can work very well in the prediction of heat transfer. In this first attempt to account for the wave effect directly, experimental data were substituted for the two wave parameters appearing in the proposed model. Future study is desirable on devising a means for the evaluation of these two parameters, either theoretically or experimentally. If such means are possible, the present theory may serve as a possible way to connect the heat transfer studies and flow dynamics studies made so far. The predicted values of the axial pressure gradient and the mean liquid film thickness have been found to agree rather well with their experimental counterparts. Therefore the present theory may be useful for the prediction of flow characteristics as well. A minor discrepancy found for the axial pressure gradient is related with thicker predicted value of liquid film thickness at large liquid flow rate.

REFERENCES

1. I. Michiyoshi, Two-phase two-component heat transfer, *Proc. 6th Int. Heat Transfer Conf.*, Vol. 6, pp. 219–234 (1978).
2. Y. Hagiwara, K. Suzuki and T. Sato, Studies on thin liquid film of annular-mist two-phase flow I. Wave characteristics and heat transfer, *Mem. Faculty of Engng Kyoto Univ.* **44**, 309–328 (1982).
3. H. Groothuis and W. P. Hendal, Heat transfer in two-phase flow, *Chem. Engng Sci.* **11**, 212–220 (1959).
4. A. A. Kudirka, R. J. Grosh and P. W. Mcfadden, Heat transfer in two-phase flow of gas–liquid mixtures, *I/EC Fundamentals* **4**, 339–344 (1965).
5. L. Fried, Pressure drop and heat transfer for two-phase two-component flow, *Chem. Engng Prog. Symp. Ser.* **50**, 47–51 (1954).
6. H. A. Johnson and A. H. Abou-Sabe, Heat transfer and pressure drop for turbulent flow of air–water mixtures in a horizontal pipe, *Trans. ASME* **74**, 977–987 (1952).
7. R. H. Pletcher and H. N. McManus, Heat transfer and pressure drop in horizontal annular two-phase two-component flow, *Int. J. Heat Mass Transfer* **11**, 1087–1104 (1968).
8. R. H. Pletcher and H. N. McManus, A theory for heat transfer to annular two-phase two-component flow, *Int. J. Heat Mass Transfer* **15**, 2091–2096 (1972).
9. A. E. Dukler, Fluid mechanics and heat transfer in vertical falling film systems, *Chem. Engng Prog. Symp. Ser.* **56**, 1–10 (1960).
10. G. F. Hewitt, *Two-Phase Flows and Heat Transfer* (edited by J. J. Ginoux), p. 111. McGraw-Hill, New York (1977).
11. D. Butterworth, An analysis of film flow and its applications to condensation in a vertical tube, *Int. J. Multiphase Flow* **1**, 671–682 (1978).
12. F. Blangetti and E. U. Schlünder, Local heat transfer coefficients on condensation in a vertical tube, *Proc. 6th Int. Heat Transfer Conf.*, Vol. 2, pp. 437–442 (1978).
13. L. K. Brumfield, R. N. Houze and T. G. Theofanous, Turbulent mass transfer at free gas–liquid interfaces with applications to film flows, *Int. J. Heat Mass Transfer* **18**, 1077–1081 (1975).
14. S. Levy and J. M. Healzer, Application of mixing length theory to wavy turbulent liquid–gas interface, *J. Heat Transfer* **103**, 492–500 (1981).
15. H. Ueda, R. Möller, S. Komori and T. Mizushina, Eddy diffusivity near the free surface of open channel flow, *Int. J. Heat Mass Transfer* **20**, 1127–1136 (1977).
16. M. Senda, K. Suzuki and T. Sato, *Turbulent Shear Flows* 2 (edited by L. J. S. Bradbury *et al.*), p. 143. Springer, Berlin (1980).
17. M. Senda and K. Suzuki, Pattern recognition study of coherent motion in a transpired turbulent boundary layer, Preprints 7th Biennial Symp. on Turbulence, No. 39 (1981).
18. W. T. Pennel, E. R. G. Eckert and E. M. Sparrow, Laminarization of turbulent pipe flow by fluid injection, *J. Fluid Mech.* **52**, 451–464 (1972).
19. B. C. Price and K. H. Bell, Design of binary vapor condensers using the Colburn–Drew equations, *A.I.Ch.E. Symp. Ser.* **70** (138), 163–171 (1974).
20. B. E. Launder and D. B. Spalding, *Mathematical Model of Turbulence*, p. 91. Academic Press, London (1972).
21. Y. Hagiwara, K. Suzuki and T. Sato, An experimental investigation on liquid droplets diffusion in annular-mist flow, in *Multi-Phase Transport: Fundamentals, Reactor Safety, Applications* (edited by N. T. Veziroglu), Vol. 1, pp. 111–131. Hemisphere, Washington (1980).
22. K. Sekoguchi *et al.*, Prepr. of Japan Soc. Mech. Eng. (in Japanese) No. 804–10, pp. 21–24 (1980).

APPENDIX

Preliminary calculations were made putting both $\tilde{\mu}_l$ and $\tilde{\mu}_g$ equal to zero. The heat transfer results of such calculations are compared with the experimental data in Fig. 6. In contrast with the good agreement found in Fig. 2, this figure shows that the calculation disregarding the wave effect gives clearly lower values for the disturbance wave conditions (symbols specified by D.W.). This may demonstrate that the present wave effect model plays an important role for disturbance waves.

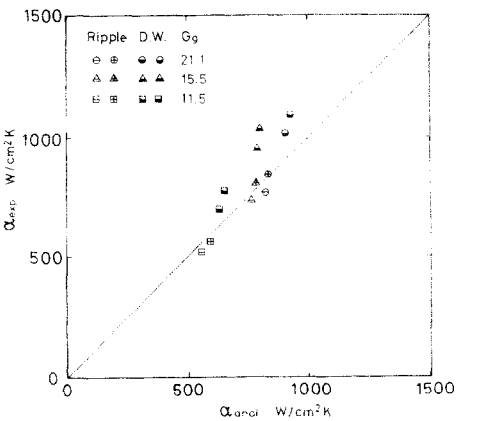

FIG. 6. Comparison of heat transfer coefficient (without considering wave effect).

UNE THEORIE DES CARACTERISTQUES D'ECOULEMENT ET DE TRANSFERT THERMIQUE DE L'ECOULEMENT ANNULAIRE DIPHASIQUE ET A DEUX COMPOSANTS

Résumé—A partir d'un modèle simple d'effet d'onde sur le transfert de quantité de mouvement, de chaleur et de masse, une théorie est proposée pour le calcul de transfert et des caractéristiques de l'écoulement annulaire diphasique et binaire. Des résultats théoriques s'accordent assez bien avec des données expérimentales obtenues pour un film liquide mince, laminaire, à surface onduleuse et chauffé à flux thermique faible.

EINE THEORIE FÜR WÄRMEÜBERGANG UND STRÖMUNGSFORMEN IN EINER ZWEIPHASEN-ZWEIKOMPONENTENSTRÖMUNG IM RINGSPALT

Zusammenfassung—Mittels eines einfachen Modells für den Einfluß von Wellen auf den Impuls-, Wärme- und Stoffübergang wird eine Theorie für die Berechnung der Wärmeübergangskoeffizienten und der Strömungsformen für eine Zweiphasen-Zweikomponentenströmung in Ringspalt vorgeschlagen. Die Ergebnisse der Berechnung stimmen gut mit den experimentellen Daten eines welligen laminaren dünnen Flüssigkeitsfilms überein, der bei geringer Wärmestromdichte beheizt wurde.

ТЕОРИЯ ТЕПЛОПЕРЕНОСА И ДИНАМИЧЕСКИХ ХАРАКТЕРИСТИК ДВУХФАЗНОГО ДВУХКОМПОНЕНТНОГО КОЛЬЦЕВОГО ПОТОКА

Аннотация—На основе простой модели влияния волнового течения на перенос импульса, тепла и массы предложена теория расчета коэффициента теплопереноса и динамических характеристик двухфазного двухкомпонентного кольцевого потока. Теоретические результаты довольно хорошо согласуются с экспериментальными данными, полученными для волнового ламинарного течения пленки жидкости при малом нагреве.